JOURNAL OF NATURAL PRODUCTS

pubs.acs.org/jnp

Article

Antimicrobial Prenylated Isoflavones from the Leaves of the Amazonian Medicinal Plant *Vatairea guianensis* Aubl.

Serhat S. Çiçek,* Mayra Galarza Pérez, Arlette Wenzel-Storjohann, Roberto M. Bezerra, Jorge F. O. Segovia, Ulrich Girreser, Isamu Kanzaki, and Deniz Tasdemir

Cite This: *J. Nat. Prod.* 2022, 85, 927−935

Read Online

ACCESS | Metrics & More | Article Recommendations | Supporting Information

ABSTRACT: *Vatairea guianenis* Aubl. (Fabaceae) is an Amazonian medicinal plant species traditionally used for treating skin diseases. In an initial screening, a *V. guianensis* leaf extract and its subextracts showed antibacterial and antifungal activities. The EtOAc subextract was selected for chemical workup and afforded five known (**1**−**4** and **8**) and six undescribed isoflavones, vatairenones C−H (**5**−**7** and **9**−**11**). All isoflavones are prenylated in position C-8, displaying either chain-prenylated (**1**−**7**) or ring-closed forms (**8**−**11**). The most bioactive compound (**3**) exhibited *in vitro* activity against clinically relevant bacteria and fungi with IC_{50} values ranging from 6.8 to 26.9 μM. Due to its broad antimicrobial activity and low general toxicity, compound **3** is a potential lead compound for structural modifications. The results of the present study support the ethnomedicinal use of *V. guianensis* in the treatment of dermatological disorders. ^{1}H NMR spectra of some of the isolated compounds showed intricate signal patterns, which might explain repeated errors in assigning the correct structure of the isoflavonoid B-ring in the literature and which we resolved by higher order spectra simulations.

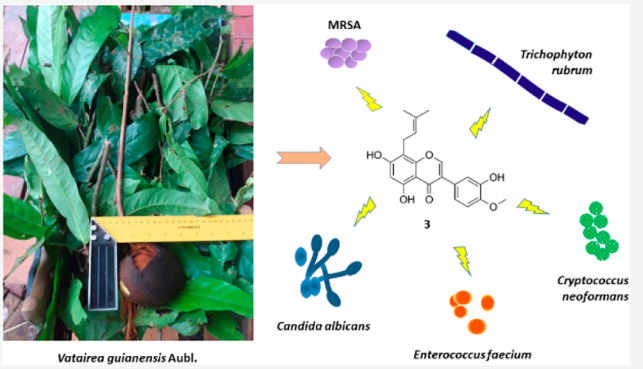

Vatairea guianensis Aubl. (Fabaceae, Papilionoideae) is a common tree in the Brazilian Amazon region, and its leaves and fruits are traditionally used for the treatment of dermatological mycosis.[1−3] The plant is commonly known as "fava de impingem", "faveira amarela", or "faveira grande do igapó" in Brazil.[2] Because of its floral morphology, the genus *Vatairea* was previously assigned to the Dalbergieae tribe, but was recently reassigned to the unranked Vataireoid clade after DNA sequence based phylogenetic analyses.[4,5] Extensive pharmacological studies were performed on *Vatairea guianensis* lectin (VGL), which was obtained from its seeds and exhibited vasorelaxant and anti-inflammatory effects.[1,6,7]

Previous phytochemical investigations on the leaves of *V. guianensis* afforded prenylated isoflavones of the derrone and lupiwighteone type, such as vatairenones A and B.[8−10] A study by de Souza et al. revealed moderate antioxidant activity for three isolated isoflavones,[8] whereas another study confirmed the antifungal activity against *Candida dublinienis* and *C. parapsilosis* of lupiwighteone (**1**) and 5,7,3′-trihydroxy-4′-methoxy-8-prenylisoflavone (**2**).[9] Da Silva et al. reported a cytotoxic effect of **1** against MCF-7 breast cancer cells, with an IC_{50} of 4.7 μM.[10] Phytochemical investigations of the sapwood did not yield prenylated isoflavonoids, but the well-known isoflavone formononetin and the isoflavanol bolusanthol D.[2] In addition, the triterpenoids lupeol, α- and β-amyrin, germanicol, and betulinic acid were detected in the leaves of *V. guianensis*.[8]

As a part of our ongoing research on Amazonian medicinal plants,[11,12] we investigated the antimicrobial potential of *V. guianensis* leaf extract. Our main aim was to find bioactive natural products to rationally support the ethnomedicinal use of this species in the treatment of dermatological ailments. Initial studies showed antibacterial and antifungal activity for the crude MeOH extract and its subextracts. In the following, we report the isolation, structure elucidation, and antimicrobial and cytotoxic effects of five known and six so far undescribed prenylated isoflavones from the EtOAc subextract of *V. guianensis* leaves.

RESULTS AND DISCUSSION

The crude MeOH extract of *V. guainensis* leaves exhibited activity against methicillin-resistant *Staphylococcus aureus* (MRSA), *Enterococcus faecium*, and *Cryptococcus neoformans*. Subsequent partitioning of the crude extract between H_2O and organic solvents of increasing polarity afforded four sub-

Received: November 2, 2021
Published: March 10, 2022

Chart 1

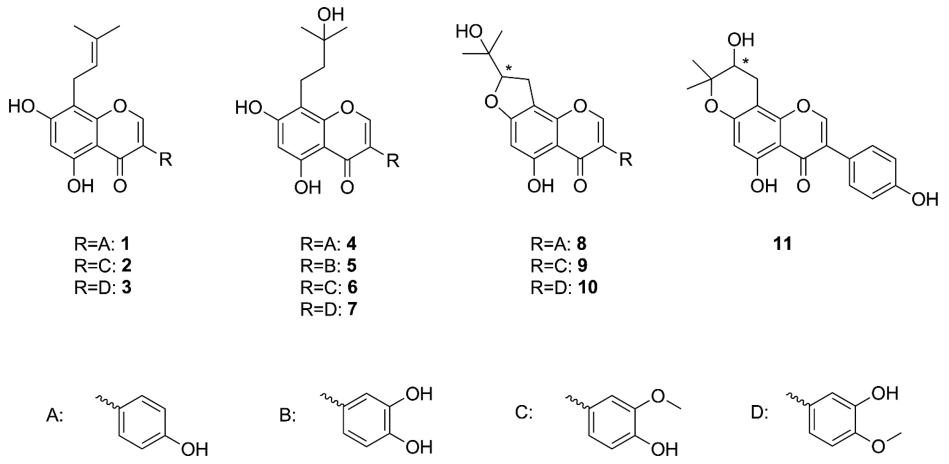

Table 1. ^{1}H NMR (400.33 MHz) Spectroscopic Data of Compounds 5, 6, 7, 9, and 11 in MeOH-d_4 (δ in ppm, J in Hz)

position	5	6	7	9	11
2	8.05, s	8.18, s	8.10, s	8.11, s	8.17, s
6	6.20, s	6.28, s	6.25, s	6.27, s	6.20, s
2′	7.01, d (2.0)	7.17, d (1.9)	7.05, m[a]	7.15, br s	7.37, d (8.6)
3′					6.84, d (8.6)
5′	6.81, d (8.3)	6.86, d (8.2)	6.96, m[a]	6.84, d (8.1)	6.84, d (8.6)
6′	6.84, dd (8.3, 2.0)	6.98, dd (8.2, 1.9)	6.96, m[a]	6.96, d (8.1)	7.37, d (8.6)
1″	2.79, m	2.81, m	2.78, m	3.25, d (8.6)	2.72, dd (16.6, 5.4)
					3.04, dd (16.6, 5.4)
2″	1.68, m	1.69, m	1.67, m	4.83, t (8.6)	3.85, t (5.4)
4″	1.27, s	1.30, s	1.28, s	1.24, s	1.37, s
5″	1.27, s	1.30, s	1.28, s	1.30, s	1.33, s
OCH_3		3.90, s	3.87, s	3.89, s	

[a]Higher order spin system (see discussion below).

Table 2. ^{13}C NMR (100.66 MHz) Spectroscopic Data of Compounds 5, 6, 7, 9, and 11 in MeOH-d_4 (δ in ppm)

position	5	6	7	9	11
2	153.2, CH	155.4, CH	156.8, CH	153.3, CH	153.4, CH
3	122.8, C	124.3, C	124.0, C	122.8, C	124.9, C
4	180.8, C	180.3, C	182.4, C	180.2, C[a]	182.5, C
5	160.0, C	159.6, C	161.3, C	164.0, C[a]	160.5, C
6	99.6, CH	99.9, CH	99.8, CH	94.8, CH	100.6, CH
7	162.0, C	160.0, C	164.1, C	168.2, C	161.1, C
8	107.8, C	108.8, C	108.7, C	106.5, C	105.8, C
9	155.6, C	155.1, C	155.1, C	154.0, C	156.5, C
10	104.9, C	104.3, C	106.0, C	104.8, C	99.8, C
1′	124.1, C	123.0, C	125.3, C	122.9, C	124.8, C
2′	114.9, CH	114.1, CH	117.3, CH	113.7, CH	131.2, CH
3′	145.4, C	146.8, C	147.4, C	148.4, C[a]	116.3, CH
4′	144.9, C	147.9, C	149.2, C	149.0, C[a]	159.3, C
5′	116.1, CH	116.4, CH	112.5, CH	116.2, CH	116.3, CH
6′	120.3, CH	114.0, CH	121.6, CH	122.6, CH	131.2, CH
1″	17.1, CH_2	18.4, CH_2	18.4, CH_2	27.3, CH_2	25.7, CH_2
2″	42.4, CH_2	43.8, CH_2	43.7, CH_2	92.8, CH	69.1, CH
3″	70.2, C	71.6, C	71.5, C	71.9, C	79.7, C
4″	27.8, CH_3	28.8, CH_3	29.2, CH_3	25.1, CH_3	25.3, CH_3
5″	27.8, CH_3	30.0, CH_3	29.2, CH_3	24.9, CH_3	21.2, CH_3
OCH_3		56.4, CH_3	56.4, CH_3	56.1, CH_3	

[a]Chemical shift values obtained from HMBC correlations.

extracts, *n*-hexane, CH_2Cl_2, EtOAc, and *n*-BuOH. The *n*-hexane subextract and the remaining H_2O layer were inactive, but all other subextracts demonstrated activity against MRSA (IC_{50} values ranging from 4.7 to 13.5 μg/mL). HPLC analysis

https://doi.org/10.1021/acs.jnatprod.1c01035
J. Nat. Prod. 2022, 85, 927−935

Table 3. ^{1}H (400.33 MHz) and ^{13}C (100.66 MHz) NMR Data of Compounds 10 and 11 in DMSO-d_6 (δ in ppm, J in Hz)

	10		11	
position	^{1}H NMR	^{13}C NMR	^{1}H NMR	^{13}C NMR
2	8.36, s	154.3, CH	8.16, s	154.5, CH
3		122.8, C		123.1, C
4		180.8, C		180.9, C
5		162.0, C		159.4, C
6	6.30, s	94.2, CH	6.25, s	99.6, CH
7		166.9, C		160.0, C
8		104.4, C		105.9, C
9		152.6, C		155.3, C
10		105.3, C		105.3, C
1′		123.9, C		121.4, C
2′	7.02, s[a]	115.6, CH	7.45, d (8.7)	130.7, CH
3′		146.7, C	6.88, d (8.7)	115.6, C
4′		148.2, C		158.2, C
5′	6.97, m[a]	112.4, CH	6.88, d (8.7)	115.6, CH
6′	6.94, m[a]	120.4, CH	7.45, d (8.7)	130.7, CH
1″	3.19, d (7.7)	26.6, CH_2	2.66, dd (16.6, 6.7); 2.98, dd (16.6, 5.1)	25.3, CH_2
2″	4.78, t (7.7)	92.0, CH	3.81, dd (6.5, 5.4)	67.2, CH
3″		70.5, C		79.4, C
4″	1.16, s	26.3, CH_3	1.32, s	25.6, CH_3
5″	1,17, s	25.3, CH_3	1.37, s	21.6, CH_3
OCH_3	3.80, s	56.2, CH_3		

[a]Higher order spin system (see discussion below).

of the bioactive subextracts indicated a similar chemical composition with varying concentrations of polar and apolar constituents. The EtOAc fraction revealed the most balanced ratio of polar and apolar metabolites and was selected for further workup. Repeated chromatographic separations yielded a series of C-8 prenylated isoflavones. Five of the 11 isolates (**1**−**4** and **8**) were identified as known natural products, whereas the remaining isoflavones are previously undescribed. In analogy to recently reported isoflavones vatairenones A and B isolated from *V. guianensis* leaves,[10] we named the undescribed compounds vatairenones C−H (**5**−**7** and **9**−**11**).

Compounds **1**−**4** and **8** were identified as lupiwighteone (**1**), 5,7,4′-trihydroxy-3′-methoxy-8-prenylisoflavone (**2**), 5,7,3′-trihydroxy-4′-methoxy-8-prenylisoflavone (**3**), lupiwighteone hydrate (**4**), and erypoegin K (**8**) by comparison of their MS and NMR spectra with literature data (Tables S1−S3).[9,13−15] Optical rotation measurements combined with chiral phase HPLC analysis suggested that the latter compound was obtained as a scalemic mixture with an enantiomeric excess of 64% of the (*R*)-isomer (Figure S105).[16] However, in the case of compound **3**, initial structural assignment by comparison with literature data afforded a rather unusual 3′,5′-substitution of the B-ring, a fact that we clarified by spectra simulations and that will be explained later on.

Compound **5** (vatairenone C) was isolated as a light yellow powder, and its molecular formula was deduced as $C_{20}H_{20}O_7$ based on HRESIMS measurements and the sodium adduct ion of m/z 395.1113 (calcd 395.1107). Analysis of the NMR data (Tables 1 and 2) indicated 20 carbon resonances, corresponding to two methyl groups (δ_C 27.8), six methane groups (δ_C 153.2, 123.6, 120.3, 116.1, 114.9, and 99.6), 10 quaternary carbons (δ_C 162.0, 160.0, 155.6, 145.4, 144.9, 124.1, 122.8, 107.8, 104.9, and 70.2), and one conjugated carbonyl carbon (δ_C 180.8). The singlet at δ_H 8.05 and the ^{13}C NMR signals at δ_C 153.2 (C-2), 122.8 (C-3), and 180.8 (C-4) were consistent with an isoflavone core structure.[17] The NMR data further showed the presence of a prenyl moiety attached to C-8 as indicated by HMBC correlations of CH_2-1″ (δ_H 2.79) to C-8 (δ_C 107.8), C-7 (δ_C 162.0), and C-9 (δ_C 155.6). The only proton of the A-ring was assigned to H-6 (δ_H 6.20) due to its HMBC correlations to C-5 (δ_C 160.0), C-7, C-9, and C-10 (δ_C 104.9). These spectroscopic data were similar to those of **4**, but suggested a different substitution pattern of the B-ring. The HRESIMS of **5** showed a molecular weight of plus 16 compared to **4** and indicated additional hydroxylation. The proton NMR spectrum, furthermore, showed the presence of two doublets, δ_H 7.02 (H-2′, J 2.0) and δ_H 6.81 (H-5′, J 8.3), which were coupling with H-6′ (δ_H 6.85) and indicated an ABX spin system for the B-ring. Thus, **5** had to be 3′,4′-*ortho*-substituted, and the structure of **5** was established as 8-(3-hydroxy-3-methylbutyl)-5,7,3′,4′-tetrahydroxyisoflavone.

Compound **6** (vatairenone D) was obtained as a yellow powder. Its molecular formula was assigned as $C_{21}H_{22}O_7$ based on HRESIMS and a sodium adduct ion of m/z 409.1267 (calcd 409.1264). Both ^{1}H and ^{13}C NMR data (Tables 1 and 2) were similar to those of **5** except for the presence of a methoxy group (δ_C 56.4, δ_H 3.89), which was also indicated by the molecular weight of plus 14. HMBC correlations of the methoxy protons with C-3′ suggested methoxylation in this position and the structure of the compound to be 8-(3-hydroxy-3-methylbutyl)-5,7,4′-trihydroxy-3′-methoxyisoflavone.

Compound **7** (vatairenone E) was obtained as light yellow powder and showed the same molecular formula ($C_{21}H_{22}O_7$) as **6** based on HRESIMS measurements and the sodium adduct ion of m/z 409.1267 (calcd 409.1264). Analysis of NMR data (Tables 1 and 2) revealed that **6** was another derivative of lupiwighteone hydrate (**4**) with a different substitution pattern in the B-ring. The presence of one hydroxy group and one methoxy group in the B-ring together with the higher order spin system also observed for compound

https://doi.org/10.1021/acs.jnatprod.1c01035
J. Nat. Prod. 2022, 85, 927−935

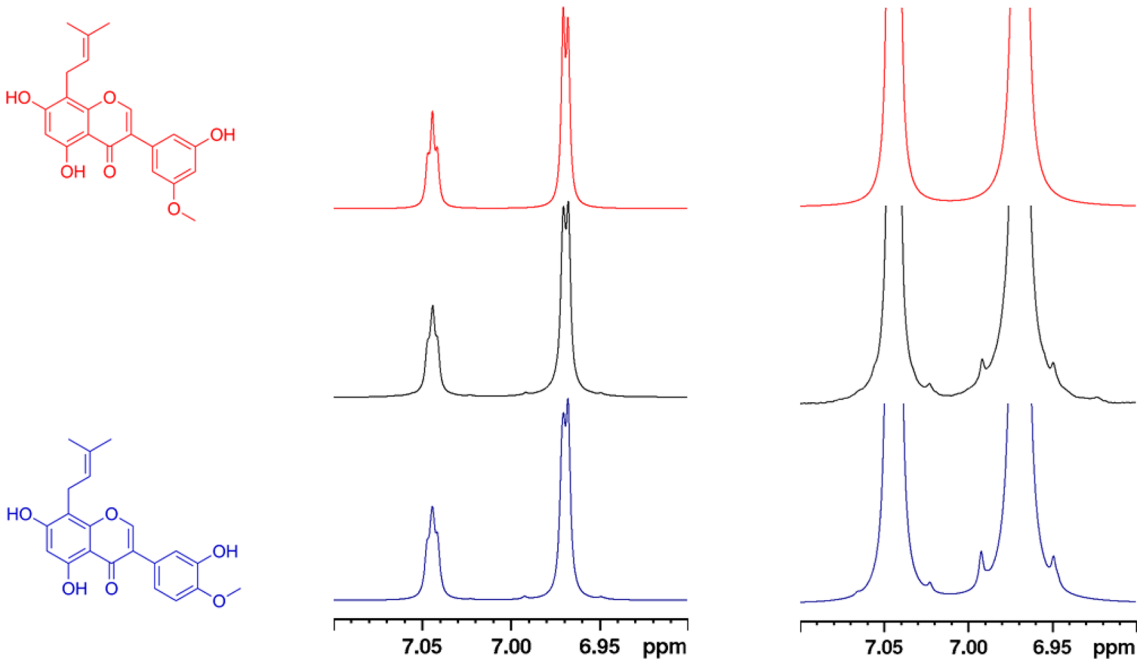

Figure 1. Expansion and enlargement of the aromatic region of the ^{1}H NMR spectrum of compound **3** in MeOH-d_4. Top: structure and simulated spectrum for a 1′,3′,5′-trisubstituted B ring, middle: measured spectrum, bottom: structure and simulated higher order spectrum for a 1′,3′,4′-trisubstituted B-ring.

3 (see discussion below) indicated a 3′-hydroxy-4′-methoxy substitution pattern and the structure of **7** to be 8-(3-hydroxy-3-methylbutyl)-5,7,3′-trihydroxy-4′-methoxyisoflavone.

Compound **9** (vatairenone F) was obtained as a light yellow powder and showed a sodium adduct ion of *m*/*z* 407.1106 (calcd for 407.1107) in the HRESIMS spectrum, corresponding to a molecular formula of $C_{21}H_{20}O_7$. Analysis of 1D and 2D NMR data (Tables 1 and 2) showed an isoflavone core structure with a hydroxyprenyl moiety in position C-8. However, compared to compounds **4**−**7**, the NMR signals of the 2″ methylene group were moved downfield from values of δ_C 42−44 and δ_H 1.7, respectively, to values of δ_C 92.8 and δ_H 4.83, indicating a neighboring oxygen atom and thus ring-closed prenylation as present in erypoegin K (**8**). The negative optical rotation ($[\alpha]^{20}_D$ −5.67) suggested an (*R*)-configuration of the compound or the respective enantiomer dominating in a scalemic mixture. The latter fact was confirmed by chiral phase HPLC analysis, where an excess of 68% of the (*R*)-enantiomer was determined (Figure S106). Moreover, the additional methoxy group as well as the coupling constants of the protons in the B-ring indicated a 4′-hydroxy-3′-methoxy substitution pattern as observed for **2** and **6**. Thus, the structure of **9** was established as 5,4′-dihydroxy-3′-methoxy-2″-hydroxyisopropyl-dihydrofurano[4,5:7,8]-isoflavone.

Compound **10** (vatairenone G) was obtained as a light yellow powder and showed the same molecular formula ($C_{21}H_{20}O_7$) as compound **9** according to a sodium adduct ion of *m*/*z* 407.1106 (calcd for 407.1107) in the HRESIMS spectrum. Analysis of the NMR data (Table 3) showed a dihydrofurylic substructure resulting from ring-closed prenylation as observed for **8** and **9**. Thus, **10** had to be another erypoegin K (**8**) derivative. Chiral phase HPLC analysis again revealed the presence of a scalemic mixture, with a ratio of 3:1 for the two isomers (enantiomeric excess of 47%) (Figure S107). A negative optical rotation value suggested that also for **10** the (*R*)-isomer was dominating in the mixture. With regard to the substitution pattern of the B-ring, compound **10** showed the same characteristics as **3** and **7**, wherefore its structure was elucidated as 5,3′-dihydroxy-4′-methoxy-2″-hydroxyisopropyl-dihydrofurano[4,5:7,8]-isoflavone.

Compound **11** (vatairenone H) was obtained as a light yellow powder, and its molecular formula was deduced as $C_{20}H_{18}O_6$ due to a sodium adduct ion *m*/*z* 377.1009 (calcd 377.1001) in the HRESIMS spectrum. Thus, **11** showed the same molecular formula as erypoegin K (**8**) as well as a negative optical rotation value ($[\alpha]^{20}_D$ −12.33). Chiral phase HPLC analysis, furthermore, revealed that compound **11** appeared as a scalemic mixture with an enantiomeric excess of 45% of the major isomer (Figure S108). Circular dichroism studies on retamasin D, the flavone counterpart of **11**, discovered negative optical rotation for the (*R*)-isomer and thus confirmed the (*R*)-enantiomer dominating in our mixture.[18] Analysis of the NMR data (Tables 1 and 2) showed values for the B-ring similar to those of **8** but different shift values for the prenyl moiety. The lower shift value of the CH-2″ methine group (δ_C 69.1 and δ_H 3.85) and the higher shift value of C-3″ (δ_C 79.7) suggested that the latter carbon was connected to the oxygen atom and that **11** showed a dihydropyrane substructure instead. This was consistent with the NMR data of vatairenone A, which was isolated in a previous study and showed the same substructure.[11] Thus, **11** was elucidated as 5,4′-dihydroxy-2″,2″-dimethyl-3″-hydroxydihydropyrano[5,6:7,8]-isoflavone.

As mentioned above, the tentative structural assignment of compound **3** (and consequently of **7** and **10**) by NMR spectroscopy and comparison with literature data afforded a prenylated isoflavone with an unusual 3′,5′-hydroxylation pattern of ring B, one of the hydroxy groups being methylated (Figure 1, top left). The measured ^{1}H and ^{13}C NMR shifts agreed well with reported values in the same NMR solvent.[19] The spin system of the three ring B protons is apparently rather simply formed by a doublet (integral two protons, H-2′

https://doi.org/10.1021/acs.jnatprod.1c01035
J. Nat. Prod. 2022, 85, 927−935

Table 4. Antimicrobial Effects of Compounds 3 and 5−7[a]

	MRSA	*E. faecium*	*C. albicans*	*C. neoformans*	*T. rubrum*
3	6.8 ± 0.3 (10.3)	12.8 ± 1.1 (5.5)	26.9 ± 2.7 (2.6)	13.6 ± 2.7 (5.1)	12.2 ± 0.3 (5.7)
5	29.6 ± 0.8 (2.9)[b]				
6	37.0 ± 1.3 (5.6)[b]	80.6 ± 2.3 (2.6)[b]			
7	49.0 ± 3.4 (>5.5)[b]				
PC	3.1 ± 0.3[b,c,d,e]	0.6 ± 0.0[b,d]	1.3 ± 0.1[b]	0.2 ± 0.0[b]	0.3 ± 0.0[b]

[a]The IC_{50} values are in μM. Selectivity index is indicated in parentheses and in italics. Positive controls (PC): chloramphenicol (MRSA), ampicillin (*E. faecium*), nystatin (*C. albicans*), amphotericin B (*C. neoformans*), clotrimazole (*T. rubrum*). Statistical significance was determined by one-way ANOVA. For $p < 0.05$ all results were statistically significant from each other. [b]$p < 0.01$ as compared with compound **3**. [c]$p < 0.01$ as compared with compound **5**. [d]$p < 0.01$ as compared with compound **6**. [e]$p < 0.01$ as compared with compound **7**.

Table 5. Cytotoxicity of Compounds 1−6[a]

	A-375	HCT-116	MB-231	HaCaT
1	88.5 ± 0.9 (1.8)	187.0 ± 10.7 (0.9)		159.8 ± 0.9
2	58.2 ± 0.5 (1.4)	109.5 ± 3.8 (1.9)	87.5 ± 1.6 (1.5)	80.7 ± 1.4
3	58.4 ± 1.6 (1.2)	87.5 ± 0.5 (0.8)	109.8 ± 8.7 (0.6)	69.8 ± 3.3
4	159.8 ± 5.6 (0.8)	222.5 ± 16.6 (1.4)	153.9 ± 11.5 (0.9)	134.6 ± 3.1
5				85.9 ± 7.4
6	250.2 ± 2.8 (0.8)	233.7 ± 5.4 (0.9)		207.0 ± 3.6
PC	0.4 ± 0.0	49.5 ± 2.2	25.8 ± 0.4	50.0 ± 1.7

[a]The IC_{50} values are in μM. Selectivity index is indicated in parentheses and italic font. Positive control (PC) was doxorubicin.

and H-6′) and a triplet (one proton, H-4′), each signal split by about 1.1 Hz. In this analysis protons H-2′ and H-6′ have the same chemical shift. The simulated spectrum is displayed in Figure 1 (top).

An expansion of the aromatic region of the measured ^{1}H NMR spectrum is shown in black (Figure 1, middle). Two differences can be observed, the asymmetric multiplets, indicating higher order effects on signal intensities, and some additional side bands next to the main signal, indicating the outer lines of a higher order spin system. They display the AB part of an ABX system, with the two protons A and B having nearly the same chemical shift and presenting the protons 5′ and 6′ of a 1′,3′,4′-trisubstituted B-ring (Figure 1, bottom left). Simulation of the chemical shifts and coupling constants afforded the spectrum shown in blue color (Figure 1, bottom). This spectrum showed the characteristics of the measured spectrum and delivered chemical shifts of 7.048 ppm for H-2′ and a chemical shift difference of only 0.005 ppm between H-5′ and H-6′ (6.795 and 6.790 ppm, respectively). The coupling constants were in the expected range (8.4 and 2.0 Hz), and an additional coupling of 0.4 Hz for H-5′ with H-2′ was considered.

Chemical shift reasoning opposes a 1′,3′,5′-trisubstituted B-ring structure as well. The value of the H-4′ proton in *ortho*-position to two hydroxy groups would be expected to be low-frequency shifted by about 0.3 to 0.5 ppm compared to the protons H-2′ and H-6′. Analysis of the ^{13}C shift values corroborates the 3′,4′-disubstitution of the B-ring. In the case of a 3′,5′-dihydroxylated or dimethoxylated B-ring, the carbon shifts are expected in the range of 155 to 160 ppm. With two substituents located at positions 3′ and 4′ the carbon shifts are in the range of 145 to 150 ppm and are only influenced to a small amount by methylation of the hydroxy substituents. The analysis of ^{1}H and ^{13}C chemical shifts in 3′,5′-disubstituted B-rings is supported by chemical shift values obtained from synthetically prepared isoflavonoids reported in the literature (Table S15).[20−22]

3′,5′-Dihydroxylated B-rings in isoflavanoids originating from plant biosynthesis are very unlikely and have been reported in the literature only about a dozen times with experimental NMR data.[23−34] Therefore, we carefully checked the reported data. The check considered (i) the employed NMR solvent and frequency, (ii) if ^{1}H or ^{13}C chemical shifts reflect the symmetry of the B-ring in 3′,5′-dihydroxy and 3′,5′-dimethoxy derivatives, (iii) ^{1}H chemical shifts of H-4′ versus H-2′ and H-6′, and (iv) ^{13}C chemical shifts of C-3′ and C-5′ as well as C-4′, respectively (Table S16).

In almost all cases, the reported structures should be re-evaluated; only one publication convincingly proved the proposed 3′,5′-substitution pattern of the B-ring.[31] Nonetheless, in many cases the higher order multiplet signals of a 3′,4′-disubstituted isoflavonoid were recognized and assigned correctly.[35,36] Due to a completely different electronic interaction, this phenomenon is not observed in the corresponding flavonoid ^{1}H NMR spectra. Here, H-6′ in ring B is high frequency shifted, compared to H-5′, and the resulting multiplets can be analyzed first order.[37]

Nine out of the 11 isolated compounds (**1**−**8** and **10**) were analyzed for their *in vitro* antimicrobial and cytotoxic potential (Tables 4 and 5). Antibacterial assays were carried out against both Gram-positive (MRSA, *Enterococcus faecium*) and Gram-negative (*Acinetobacter baumannii*) bacteria. Antifungal activity was evaluated against *Candida albicans*, *Cryptococcus neoformans*, and the dermatophyte *Trichophyton rubrum*. In addition, cytotoxicity was assessed against three human cancer lines, melanoma (A-375), colon cancer (HCT-116), and human breast cancer (MB-231). General toxicity was assessed employing the noncancerous human keratinocyte cell line (HaCaT). Cut-off values for both antimicrobial and cytotoxicity assays were defined with 100 μg/mL; that is, IC_{50} values were only determined for compounds with more than 50% inhibition at this concentration.

Only four compounds (**3** and **5**−**7**) exhibited activity against MRSA, with compound **3** being the most potent (IC_{50} value of 6.8 μM) (Table 4). Notably, all active compounds showed

https://doi.org/10.1021/acs.jnatprod.1c01035
J. Nat. Prod. 2022, 85, 927−935

chain-open prenylation, while none of the compounds with ring-closed isoprene moieties were effective. Two compounds were active against *E. faecium*, with **3** again being the most effective compound (IC_{50} value 12.8 μM). In contrast, compound **6** showed only weak activity (IC_{50} value of 80.6 μM). A similar pattern was observed in the antifungal assays against *C. albicans*, *C. neoformans*, and *T. rubrum*. Here, only **3** displayed activity, with IC_{50} values of 26.9, 13.6, and 12.2 μM, respectively. Thus, compound **3** showed activity against five out of the six tested microbial test strains. The fact that **3** was active against MRSA and *T. rubrum*, which both cause dermatological disorders, furthermore corroborates the ethnomedicinal use of *V. guianensis* leaves.

Cytotoxic effects of the tested compounds were lower and less differentiated, with most of the tested compounds showing no or only weak effects against cancer cell lines (Table 5). Moderate activities were observed for **1**−**3** against human malignant melanoma (A-375) cells with IC_{50} values of 88.5, 58.2, and 58.4 μM, respectively. Compounds **2** and **3** exhibited marginal activity toward MB-231 and HCT-116 cells with the same IC_{50} value of 87.5 μM. Except for **1**, all compounds (**2**, **3**, and **5**) showed significant toxicity against the HaCaT cell line. Notably, **3** displays a selectivity index (SI) of 10 against MRSA and an SI of 5 against *E. faecium*, *C. neoformans*, and *T. rubrum*, respectively.

Isoflavonoids and especially prenylated isoflavonoids are known to exhibit various biological effects.[38] A previous study on the osteogenic activities of genistein and its derivatives found that diprenylation in positions C-6 and C-8 increases the bone protective effects, which were more pronounced when prenylation occurred at C-8.[39] A screening for antitumor promotors toward Epstein−Barr virus activation, furthermore, showed that single or double prenylation increased the compounds' inhibitory activity.[40] Glabridin, one of the most investigated prenylated isoflavonoids, has been shown to induce apoptosis in leukemia cells,[41] a fact that was also found for (*S*)-erypoegin K,[16] which was part of the scalemic erypoegin K (**8**) mixture obtained in our study. With regard to the antibacterial activity of complex isoflavonoids, a study on the legume seedling extracts found the effect against *Listeria monocytogenes* and MRSA correlating with the total content of C-6-prenylated compounds rather than with compounds prenylated in position C-8 or C-3′.[42]

Our study showed that also C-8-prenylated isoflavonoids demonstrate notable antibacterial activity, not only against MRSA but also against other clinically relevant strains. With respect to the antifungal activity, Souza et al. reported pronounced activity for the EtOAc-soluble portion of the crude ethanolic extract of *V. guianensis* leaves against four *Candida* species.[9] However, two isolated major components (**1** and **3**) affected only two of the investigated *Candida* species and were not active against *C. albicans* and *C. krusei*. Compound **1** also exhibited no effect against *C. albicans* in our study, whereas **3** was significantly active.

In summary, the present study revealed a series of complex isoflavones, of which six compounds (**5**−**7** and **9**−**11**) were identified as previously undescribed natural products. One of the isolated constituents (**3**) exhibited inhibitory effects against two clinically relevant bacterial and three fungal strains. Its broad antimicrobial activity and relatively low cytotoxicity render compound **3** a potential candidate for further optimization by a medicinal chemistry approach. With the activity against two strains that cause dermatological disorders, our study, furthermore, corroborates the ethnomedicinal use of *V. guianensis* for treating skin diseases. Because of the restricted occurrence of isoflavones in the plant kingdom and the increasing use of prenylated flavonoids for the development of new therapeutic agents,[43] *V. guianensis* presents a source of valuable natural products. Apart from our phytopharmacological findings, our study revealed deceptive coupling patterns in the proton NMR spectra observed for 3′,4′-disubstituted isoflavonoids, which have been the reason for several erroneously reported structures and which we resolved by higher order spectra simulations.

EXPERIMENTAL SECTION

General Experimental Procedures. Thin layer chromatography was performed with precoated TLC plates (silica gel 60 F254 Merck, Germany) using either EtOAc−MeOH−H_2O (10:1:1.5, TLC system 1), CH_2Cl_2−MeOH (10:1, TLC system 2), or CH_2Cl_2−MeOH (10:2, TLC system 3) as eluents and vanillin sulfuric acid as spraying reagent. Flash chromatography was carried out with a Büchi PrepChrom C-700 chromatograph using a FlashPure EcoFlex silica gel SL cartridge (100 g/135 mL, irregular 40−63 μm particle size, Büchi Labortechnik GmbH, Essen, Germany). Column chromatography was performed with Sephadex LH-20 (GE Healthcare AB, Uppsala, Sweden). Semipreparative HPLC was accomplished using a Waters Alliance e2695 separations module with an Alliance 2998 photodiode array detector and a WFC III fraction collector (Waters, Milford, MA, USA) using a Phenomenex Aqua C18 column (250 × 10 mm, 5 μm particle size, Phenomenex, Aschaffenburg, Germany). HPLC-UV analyses were performed on an Ultimate 3000 chromatograph equipped with an HPG-3400SD pump, connected to a WPS-3000SL autosampler, TCC-3000SD column heater, and a VWD-3400RS variable-wavelength detector (Thermo Scientific, Waltham, MA, USA). UHPLC-DAD-MS analyses were carried out on a Shimadzu Nexera 2 liquid chromatograph connected to an LC-MS triple quadrupole mass spectrometer using electrospray ionization (Shimadzu, Kyoto, Japan). A Phenomenex Luna Omega C18 column (100 × 2.1 mm, 1.6 μm particle size, Phenomenex, Aschaffenburg, Germany) was employed for the analysis of extracts, fractions, and pure compounds. Chiral phase HPLC analysis was performed on a Lux Amylose-1 column (250 × 4.6 mm, 3 μm particle size, Phenomenex, Aschaffenburg, Germany). Melting points were measured on a Stuart SMP30 melting point apparatus (Cole-Palmer, Staffordshire, UK) using glass melting point tubes. IR spectra were recorded on a Spectrum 100 FT-IR spectrometer (PerkinElmer, Waltham, MA, USA) using attenuated total reflection. All compounds were measured as solids except compounds **5**, **9**, and **11**, which were applied as methanolic solutions and measured as films. High-resolution MS spectra were recorded on a micrOTOF II-High-performance TOF-MS system equipped with an electrospray ionization source (Bruker, Billerica, MA, USA). Specific rotation of the compounds was measured on a Jasco P-2000 polarimeter (Jasco, Pfungstadt, Germany). 1D (^{1}H, ^{13}C) and 2D (HSQC, HMBC, COSY, NOESY) NMR spectra were recorded on a Bruker Avance III 400 NMR spectrometer operating at 400 MHz for the proton channel and 100 MHz for the ^{13}C channel with a 5 mm PABBO broad band probe with a z gradient unit at 298 K (Bruker BioSpin GmbH, Rheinstetten, Germany). Reference values were 2.09 (^{1}H) and 205.87 (^{13}C) for acetone, 2.50 (^{1}H) and 39.51 ppm (^{13}C) for dimethyl sulfoxide, and 3.31 (^{1}H) and 49.15 ppm (^{13}C) for MeOH, respectively. Structure elucidation and spectra simulations were performed using Topspin 3.6 software (Bruker Biospin GmbH, Rheinstetten, Germany). Conventional 5 mm NMR sample tubes were obtained from Rototec-Spintec GmbH (Griesheim, Germany).

Chemical Reagents. LC-MS grade formic acid was purchased from Sigma-Aldrich Co. (St. Louis, MO, USA). LC-MS grade MeCN, isopropanol, *n*-hexane, H_2O, gradient grade MeOH, and other (analytical grade) solvents were obtained from VWR International GmbH (Darmstadt, Germany). H_2O used for isolation was doubly

https://doi.org/10.1021/acs.jnatprod.1c01035
J. Nat. Prod. 2022, 85, 927−935

distilled in-house. DMSO-d_6 (99.80%, lot S1051, batch 0119E) and MeOH-d_4 (99.80%, lot P3021, batch 1016B) for NMR spectroscopy were purchased from Euriso-top GmbH (Saarbrücken, Germany).

Plant Material. Leaves of *V. guianensis* were collected in April 2020 at the coordinates N 00° 13′30.3″/W 051° 33′24.2″ and identified by Jorge F. O. Segovia. A voucher specimen is kept in EMBRAPA under the registration number BRM 027. The species was registered for access to the genetic heritage in SisGen with the process no. 00.038.174/0001-43.

Extraction and Isolation. Dried and ground leaves (628.5 g) were extracted five times with 2 L of MeOH using ultrasonication for 15 min followed by maceration for at least 12 h to yield 137.9 g of crude extract after evaporation of the solvent. The crude MeOH extract was suspended in H_2O and subsequently extracted with CH_2Cl_2 and EtOAc, giving 44.69 g of CH_2Cl_2 subextract, 27.24 g of EtOAc subextract, and 49.58 g of residue after evaporation of the aqueous layer.

For further separation, a portion (10.44 g) of the EtOAc subextract was subjected to flash chromatography using silica gel as stationary phase and a gradient going from 100% *n*-hexane to 100% EtOAc in 25 min and to 100% MeOH in another 25 min. Flow rate was set to 50 mL/min, and 100 fractions of 25 mL were collected. Fractions were combined according to their similarity based on TLC analyses, affording a total of 10 fractions (A−J).

Fraction B (1.326 g) was further separated using Sephadex LH-20 chromatography (100 × 2.5 cm) and acetone as solvent to give 112 fractions, which were combined to four fractions (B1−B4) according to results of TLC system 2. Fraction B2 (vials 34−47, 439.2 mg) was subjected to the same column, yielding 145 vials, which were combined using TLC system 3 to yield five fractions (B2A−B2E). Fraction B2D (vials 73−90) consisted of 84.1 mg of **1**, and fraction B2B yielded 6.90 mg of **2** and 21.4 mg of **3** after separation with semipreparative HPLC using H_2O−MeCN (50:50) as eluent and peak collection from 26.8 to 29.1 min and 29.2 to 33.0 min, respectively, at a temperature of 40 °C.

Fraction E (781 mg) was also subjected to Sephadex LH-20 chromatography (100 × 2.5 cm, acetone), giving 228 vials, which were combined to 10 fractions (E1−E10) according to results of TLC system 3. Fraction E7 (vials 93−112, 43.9 mg) yielded 4.70 mg of **5** after purification by semipreparative HPLC using H_2O−MeCN (70:30 at 40 °C) and peak collection from 18.4 to 23.0 min. Fraction E5 (141.1 mg) was chromatographed over Sephadex LH-20 material (170 × 2.5 cm, MeOH) to yield 60.5 mg of **4**. Fraction E4 (90.2 mg) was subjected to semipreparative HPLC applying H_2O−MeCN (65:35) as eluent and a separation temperature of 40 °C to give 5.10 mg of **6** (22.5 to 24.3 min) and 21.7 mg of **7** (24.4 to 27.4 min). Fraction E3 (67.6 mg) was chromatographed by semipreparative HPLC using H_2O−MeCN (60:40 at 40 °C) and yielded 2.60 mg of **8** (22.5 to 24.3 min), 4.20 mg of compound **10** (26.6 to 28.0 min), and 4.71 mg of a mixture of compounds **9** and **11**. After NMR spectroscopy the mixture was separated by Sephadex LH-20 chromatography (100 × 1 cm, MeOH) using LC-MS for peak differentiation to give 1.26 mg of **9** and 1.88 mg of **11**.

*Lupiwighteone (**1**):* light yellow powder; mp 144 °C; LC-UV [0.1% formic acid in H_2O−MeCN (35:65)] λ_{max} 224, 264 (Figure S1); HRESIMS (positive) m/z 339.1226 $[M + H]^+$ (calcd for $C_{20}H_{19}O_5$, 339.1232) and 361.1043 $[M + Na]^+$ (calcd for $C_{20}H_{18}O_5Na$, 361.1052) (Figure S3); ^1H NMR (MeOH-d_4 and DMSO-d_6, 400 MHz) and ^{13}C NMR (MeOH-d_4 and DMSO-d_6, 100 MHz) see Tables S1−S3 and Figures S4−S13, Supporting Information.

*5,7,4′-Trihydroxy-3′-methoxy-8-prenylisoflavone (**2**):* light yellow powder; mp 156 °C; LC-UV [0.1% formic acid in H_2O−MeCN (35:65)] λ_{max} 220, 265 (Figure S14); HRESIMS (positive) m/z 391.1161 $[M + Na]^+$ (calcd for $C_{21}H_{20}O_6Na$, 391.1158) (Figure S16); ^1H NMR (MeOH-d_4, 400 MHz) and ^{13}C NMR (MeOH-d_4, 100 MHz) see Tables S1 and S3 and Figures S17−S21, Supporting Information.

*5,7,3′-Trihydroxy-4′-methoxy-8-prenylisoflavone (**3**):* light yellow powder; mp 163 °C; LC-UV [0.1% formic acid in H_2O−MeCN (35:65)] λ_{max} 224, 265 (Figure S22); HRESIMS (positive) m/z = 391.1162 $[M + Na]^+$ (calcd for $C_{21}H_{20}O_6Na$, 391.1158) (Figure S24); ^1H NMR (MeOH-d_4 and DMSO-d_6, 400 MHz) and ^{13}C NMR (MeOH-d_4 and DMSO-d_6, 100 MHz) see Tables S1−S3 and Figures S25−S34, Supporting Information.

*Lupiwighteone hydrate (**4**):* yellow powder; mp 244 °C (degradation); LC-UV [0.1% formic acid in H_2O−MeCN (60:40)] λ_{max} 264 (Figure S33); HRESIMS (positive) m/z = 357.1343 $[M + H]^+$ (calcd for $C_{20}H_{21}O_6$, 357.1338) and 379.1167 $[M + Na]^+$ (calcd for $C_{20}H_{20}O_6Na$, 379.1158) (Figure S35); ^1H NMR (MeOH-d_4 and DMSO-d_6, 400 MHz) and ^{13}C NMR (MeOH-d_4 and DMSO-d_6, 100 MHz) see Tables S1−S3 and Figures S36−S45, Supporting Information. Compound **4** was isolated as a still impure sample.

*Vatairenone C (**5**):* light yellow powder; mp 262 °C (degradation); LC-UV [0.1% formic acid in H_2O−MeCN (70:30)] λ_{max} 231, 264 (Figure S46); HRESIMS (positive) m/z 395.1113 $[M + Na]^+$ (calcd for $C_{20}H_{20}O_7Na$, 395.1107) (Figure S48); ^1H NMR (MeOH-d_4, 400 MHz) and ^{13}C NMR (MeOH-d_4, 100 MHz) see Tables 1 and 2 and Figures S49−S53, Supporting Information.

*Vatairenone D (**6**):* yellow powder; mp 256 °C (degradation); LC-UV [0.1% formic acid in H_2O−MeCN (60:40)] λ_{max} 231, 264 (Figure S54); HRESIMS (positive) m/z 409.1267 $[M + Na]^+$ (calcd for $C_{21}H_{22}O_7Na$, 409.1264) (Figure S55); ^1H NMR (MeOH-d_4, 400 MHz) and ^{13}C NMR (MeOH-d_4, 100 MHz) see Tables 1 and 2 and Figures S56−S61, Supporting Information. Compound **6** was obtained as a still impure sample.

*Vatairenone E (**7**):* light yellow powder; mp 238 °C (degradation); LC-UV [0.1% formic acid in H_2O−MeCN (60:40)] λ_{max} 229, 265 (Figure S62); HRESIMS (positive) m/z 409.1267 $[M + Na]^+$ (calcd for $C_{21}H_{22}O_7Na$, 409.1264) (Figure S64); ^1H NMR (MeOH-d_4, 400 MHz) and ^{13}C NMR (MeOH-d_4, 100 MHz) see Tables 1 and 2 and Figures S65−S69, Supporting Information.

*Erypoegin K (**8**):* light yellow powder; mp 252 °C; $[\alpha]^{20}_D$ −46.80 (*c* 0.3, MeOH); LC-UV [0.1% formic acid in H_2O−MeCN (60:40)] λ_{max} 227, 264 (Figure S70); HRESIMS (positive) m/z 377.1005 $[M + Na]^+$ (calcd for $C_{20}H_{18}O_6Na$, 377.1001) (Figure S72); ^1H NMR (DMSO-d_6, 400 MHz) and ^{13}C NMR (DMSO-d_6, 100 MHz) see Tables S1 and S2 and Figures S73−S78, Supporting Information.

*Vatairenone F (**9**):* light yellow powder; mp 218 °C; $[\alpha]^{20}_D$ −5.67 (*c* 0.1, MeOH); LC-UV [0.1% formic acid in H_2O−MeCN (60:40)] λ_{max} 263 (Figure S79); HRESIMS (positive) m/z 407.1106 $[M + Na]^+$ (calcd for $C_{21}H_{20}O_7Na$, 407.1107) (Figure S81); ^1H NMR (MeOH-d_4, 400 MHz) and ^{13}C NMR (MeOH-d_4, 100 MHz) see Tables 1 and 2 and Figures S82−S87, Supporting Information.

*Vatairenone G (**10**):* light yellow powder; mp 239 °C; $[\alpha]^{20}_D$ −26.73 (*c* 0.1, MeOH); LC-UV [0.1% formic acid in H_2O−MeCN (60:40)] λ_{max} 229, 265 (Figure S88); HRESIMS (positive) m/z 407.1102 $[M + Na]^+$ (calcd for $C_{21}H_{20}O_7Na$, 407.1107) (Figure S90); ^1H NMR (DMSO-d_6, 400 MHz) and ^{13}C NMR (DMSO-d_6, 100 MHz) see Tables 1 and 2 and Figures S91−S96, Supporting Information.

*Vatairenone H (**11**):* light yellow powder; mp 222 °C; $[\alpha]^{20}_D$ −12.33 (*c* 0.1, MeOH); LC-UV [0.1% formic acid in H_2O−MeCN (60:40)] λ_{max} 242, 264 (Figure S97); HRESIMS (positive) m/z 377.1009 $[M + Na]^+$ (calcd for $C_{20}H_{18}O_6Na$, 377.1001) (Figure S98); ^1H NMR (MeOH-d_4 and DMSO-d_6, 400 MHz) and ^{13}C NMR (MeOH-d_4 and DMSO-d_6, 100 MHz) see Tables 1−3 and Figures S82−S87 and S100−S104, Supporting Information.

Biological Activity. Antibacterial and antifungal activity testing of all samples was performed as described by Çiçek et al.[12] Cytotoxicity and antidermatophytic assays were conducted as described by Pfeifer Barbosa et al.[11] Selectivity indices were calculated using the results obtained from human keratinocyte cell line HaCaT. For compound **7**, which showed no activity against HaCaT cells, the selectivity index was calculated using a concentration of 259 μM (corresponding to the cutoff value of 100 μg/mL).

https://doi.org/10.1021/acs.jnatprod.1c01035
J. Nat. Prod. 2022, 85, 927−935

■ ASSOCIATED CONTENT

Supporting Information

The Supporting Information is available free of charge at https://pubs.acs.org/doi/10.1021/acs.jnatprod.1c01035.

^{1}H and ^{13}C NMR data of **1**−**4** and **8**; UV, IR, HRESIMS, and 1D and 2D NMR spectra of **1**−**11**; chromatograms of chiral phase HPLC analysis (PDF)

■ AUTHOR INFORMATION

Corresponding Author

Serhat S. Çiçek − *Department of Pharmaceutical Biology, Kiel University, 24118 Kiel, Germany;* orcid.org/0000-0002-3038-8523; Phone: +49 431 880 1077; Email: scicek@pharmazie.uni-kiel.de

Authors

Mayra Galarza Pérez − *Department of Pharmaceutical Biology, Kiel University, 24118 Kiel, Germany*

Arlette Wenzel-Storjohann − *GEOMAR Centre for Marine Biotechnology (GEOMAR-Biotech), Research Unit Marine Natural Products Chemistry, GEOMAR Helmholtz Centre for Ocean Research Kiel, 24106 Kiel, Germany*

Roberto M. Bezerra − *Laboratory of Bioprospection and Atomic Absorption, Federal University of Amapá, Macapá 68903-419 Amapá, Brazil*

Jorge F. O. Segovia − *Brazilian Agricultural Research Corporation, Ecoregional Research Unit, Macapá 68903-419 Amapá, Brazil*

Ulrich Girreser − *Department of Pharmaceutical and Medicinal Chemistry, Kiel University, 24118 Kiel, Germany*

Isamu Kanzaki − *Laboratory of Bioprospection, University of Brasilia, 70910-900 Brasilia, DF, Brazil*

Deniz Tasdemir − *GEOMAR Centre for Marine Biotechnology (GEOMAR-Biotech), Research Unit Marine Natural Products Chemistry, GEOMAR Helmholtz Centre for Ocean Research Kiel, 24106 Kiel, Germany; Kiel University, 24118 Kiel, Germany;* orcid.org/0000-0002-7841-6271

Complete contact information is available at: https://pubs.acs.org/10.1021/acs.jnatprod.1c01035

Notes

The authors declare no competing financial interest.

■ ACKNOWLEDGMENTS

The authors thank Claudia Welsch (GEOMAR-Biotech) for HRESIMS and optical rotation measurements, Prof. Christian Zidorn for proof reading, and the Federal District Funding Agency/FAP DF, Brazil, for partially funding the work.

■ REFERENCES

(1) Silva, H. C.; Nagano, C. S.; Souza, L. A. G.; Nascimento, K. S.; Isídro, R.; Delatorre, P.; Rocha, B. A. M.; Sampaio, A. H.; Assreuy, A. M. S.; Pires, A. F.; Damasceno, L. E. A.; Marques-Domingos, G. F. O.; Cavada, B. S. *Process Biochem.* **2012**, *47*, 2347−2355.

(2) de Souza, R. F.; da Silva, J. K. R.; da Silva, G. A.; Arruda, A. C.; da Silva, M. N.; Arruda, M. S. P. *Rev. Virtual Quim.* **2015**, *7*, 1893−1906.

(3) Oliveira, A. A.; Segovia, J. F. O.; Sousa, V. Y. K.; Mata, E. C. G.; Gonçalves, M. C. A.; Bezerra, R. M.; Junior, P. O. M.; Kanzaki, L. I. B. *SpringerPlus* **2013**, *2*, 371.

(4) Cardoso, D.; de Queiroz, L. P.; de Lima, H. C.; Suganuma, E.; van den Berg, C.; Lavin, M. *Am. J. Bot.* **2013**, *100*, 403−421.

(5) Cardoso, D.; Pennington, R. T.; de Queiroz, L. P.; Boatwright, J. S.; van Wyk, B.-E.; Wojciechowski, M. F.; Lavin, M. *S. Afric. J. Bot.* **2013**, *89*, 58−75.

(6) Marques, G. F. O.; Osterne, V. J. S.; Almeida, L. M.; Oliveira, M. V.; Brizeno, L. A. C.; Pinto-Junior, V. R.; Santiago, M. Q.; Neco, A. H. B.; Mota, M. R. L.; Souza, L. A. G.; Nacimento, K. S.; Pires, A. F.; Cavada, B. S.; Assreuy, A. M. S. *Biochimie* **2017**, *140*, 58−65.

(7) Marques, G. F. O.; Pires, A. F.; Osterne, V. J. S.; Pinto-Junior, V. R.; Silva, I. B.; Martins, M. G. Q.; Oliveira, M. V.; Gomes, A. M.; de Souza, L. A. G.; Pavão, M. S. G.; Cavada, B. S.; Assreuy, A. M. S.; Nascimento, K. S. *J. Mol. Recognit.* **2021**, *34*, e2922.

(8) de Souza, R. F.; Marinho, V. H. S.; da Silva, G. A.; Costa, L. M.; da Silva, J. K. R.; Bastos, G. N. T.; Arruda, A. C.; da Silva, M. N.; Arruda, M. S. P. *J. Braz. Chem. Soc.* **2013**, *24*, 1857−1863.

(9) Souza, R. F.; da Silva, G. A.; Arruda, A. C.; da Silva, M. N.; Santos, A. S.; Grisolia, D. P. A.; Silva, M. B.; Salgado, C.; Arruda, M. S. P. *J. Braz. Chem. Soc.* **2016**, *28*, 1132−1136.

(10) Da Silva, G. A.; de Souza, R. F.; Marinho, V. H.; Pinheiro, W. B.; Pinto, L. C.; Montenegro, R. C.; Arruda, A. C.; Silva, M. N.; Arruda, M. S. *Sci. Plena* **2020**, *16*, 117201.

(11) Pfeifer Barbosa, A. L.; Wenzel-Storjohann, A.; Diomedes Barbosa, J.; Zidorn, C.; Peifer, C.; Tasdemir, D.; Çiçek, S. S. *J. Ethnopharmacol.* **2019**, *233*, 94−100.

(12) Çiçek, S. S.; Wenzel-Storjohann, A.; Girreser, U.; Tasdemir, D. *Rev. Bras. Farmacogn.* **2020**, *30*, 18−27.

(13) Ji, S.; Li, Z.; Song, W.; Wang, Y.; Liang, W.; Li, K.; Tang, S.; Wang, Q.; Qiao, X.; Zhou, D.; Yu, S.; Ye, M. *J. Nat. Prod.* **2016**, *79*, 281−292.

(14) Hashidoko, Y.; Tahara, S.; Mizutani, J. *Agric. Biol.Chem.* **1986**, *50*, 1797−1807.

(15) Dai, J.; Shen, D.; Yoshida, W. Y.; Parrish, S. M.; Williams, P. G. *Planta Med.* **2012**, *78*, 1357−1362.

(16) Hikita, K.; Saigusa, S.; Takeuchi, Y.; Matsuyama, H.; Nagai, R.; Kato, K.; Murata, T.; Tanaka, H.; Wagh, Y. S.; Asao, N.; Kaneda, N. *Bioorg. Med. Chem.* **2020**, *28*, 115940.

(17) Deyou, T.; Marco, M.; Heydenreich, M.; Pan, F.; Gruhonjic, A.; Fitzpatrick, P. A.; Koch, A.; Derese, S.; Pelletier, J.; Rissanen, K.; Yenesew, A.; Erdélyi, M. *J. Nat. Prod.* **2017**, *80*, 2060−2066.

(18) Nur-e-Alam, M.; Yousaf, M.; Parveen, I.; Hafizur, R. M.; Ghani, U.; Ahmed, S.; Hameed, A.; Threadgillb, M. D.; Al-Rehaily, A. J. *Org. Biomol. Chem.* **2019**, *17*, 1266−1276.

(19) Tchize Ndejouong, B.; Le, S.; Sattler, I.; Dahse, H.-M.; Kothe, E.; Hertweck, C. *Bioorg. Med. Chem. Lett.* **2009**, *19*, 6473−6476.

(20) Klier, L.; Bresser, T.; Nigst, T. A.; Karaghiosoff, K.; Knochel, P. *J. Am. Chem. Soc.* **2012**, *134*, 13584−13587.

(21) Lee, J. I. *Bull. Korean Chem. Soc.* **2016**, *37*, 1132−1135.

(22) Mkrtchyan, S.; Iaroshenko, V. O. *Chem. Commun.* **2020**, *56*, 2606−2609.

(23) Xuan, B.; Du, X.; Li, X.; Shen, Z. *Nat. Prod. Res.* **2016**, *30*, 1423−1430.

(24) Vitor, R. F.; Mota-Filipe, W.; Teixeira, G.; Borges, C.; Rodrigues, A. I.; Teixeira, A.; Paulo, A. *J. Ethnopharm.* **2004**, *93*, 363−370.

(25) Simões, M. A. M.; Pinto, D. C. G. A.; Neves, B. M. R.; Silva, A. M. S. *Molecules* **2020**, *25*, 812.

(26) Yang, R.-Y.; Lan, Y.-S.; Huang, Z.-J.; Shao, C.-L.; Liang, H.; Chen, Z.-F.; Li, J. *Chem. Nat. Compd.* **2012**, *48*, 674−676.

(27) Shrestha, S. P.; Narukawa, Y.; Takeda, T. *Chem. Pharm. Bull.* **2007**, *55*, 926−929.

(28) Wang, G.-R.; Tang, W.-Z.; Yao, Q.-Q.; Zhong, H.; Liu, Y.-J. *J. Nat. Med.* **2010**, *64*, 358−361.

(29) Tianjin University of Science and Technology, Chinese Patent 106589019 A, 2016.

(30) El-Latif, A. R. R.; Shabana, M. H.; El-Gandour, A. H.; Mansour, R. M.; Sharaf, M.; *Chem. Nat. Compd.* **2003**, *39*, 536−537.

(31) Kovalev, V. N.; Zatyl'nikova, O. A.; Kovalev, S. V. *Chem. Nat. Compd.* **2013**, *49*, 34−35.

(32) Shen, H.; Sun, J.; Zhao, P.; Tang, M.; Liu, Y.; Xia, P. *Chem. Nat. Compd.* **2014**, *50*, 621−623.

(33) Tianjin University of Science and Technology, Chinese Patent 105646621A, 2016.
(34) Scribuhom, T.; Thongsri, Y.; Yenjai, C. *Asian J. Chem.* **2020**, *32*, 1788−1792.
(35) Chiang, C.-M.; Chang, Y.-J.; Wu, J.-Y.; Chang, T.-S. *Molecules* **2017**, *22*, 87.
(36) Li, S.; Liu, C.; Zhang, Y.; Tsao, R. *Phytochem. Anal.* **2021**, *32*, 640−653.
(37) Yamauchi, K.; Mitsunaga, T.; Itakura, Y.; Batubara, I. *Fitoterapia* **2015**, *104*, 69−74.
(38) Botta, B.; Menendez, P.; Zappia, G.; de Lima, R. A.; Torge, R.; delle Monachea, G. *Curr. Med. Chem.* **2009**, *16*, 3414−3468.
(39) Zhang, Y.; Li, X.-L.; Yao, X.-S.; Wong, M.-S. *Arch. Pharm. Res.* **2008**, *31*, 1534−1539.
(40) Ito, C.; Itoigawa, M.; Tan, H. T.; Tokuda, H.; Yang Mou, X.; Mukainaka, T.; Ishikawa, T.; Nishino, H.; Furukawa, H. *Cancer Lett.* **2000**, *152*, 187−192.
(41) Huang, H.-L.; Hsieh, M.-J.; Chien, M. H.; Chen, H.-Y.; Yang, S.-F.; Hsiao, P.-C. *PLoS One* **2014**, *9*, e98943.
(42) Araya-Cloutier, C.; den Besten, H. M. W.; Aisyah, S.; Gruppen, H.; Vincken, J.-P. *Food Chem.* **2017**, *226*, 193−201.
(43) Shi, S.; Li, J.; Zhao, X.; Liu, Q.; Song, S.-J. *Phytochemistry* **2021**, *191*, 112895.

https://doi.org/10.1021/acs.jnatprod.1c01035
J. Nat. Prod. 2022, 85, 927−935